A FULLY SELF-SUFFICIENT ENERGY HARVESTING SYSTEM FOR HUMAN MOVEMENTS

Yuan Rao, Shuo Cheng, and David P. Arnold
Interdisciplinary Microsystems Group, Dept. Electrical and Computer Eng., University of Florida, USA

Abstract: This paper presents a complete, self-contained energy harvesting system that converts motion from daily human activities, such as walking, jogging, and cycling, into usable electrical energy. The system requires no external power supplies and features zero standby power when the input motion is too small for successful energy reclamation. When attached to a person's ankle during walking, the 100 cm^3 prototype is shown to charge a 3.7 V lithium-ion polymer battery at an average power of 300 μW. The design and testing of the system under other operating conditions are presented herein.

Keywords: energy harvesting system, magnetic energy harvester, interface circuit, human movement

INTRODUCTION

Achieving autonomous, self-sustaining, and maintenance-free operation while avoiding battery replacement or recharge has become an increasingly important topic in the development of modern wireless systems. One promising solution to this problem is to build self-powered systems using energy harvesting techniques. Although the energy harvesting approach adds complexity to the implementation of a system, it provides the possible benefit of making the system completely self-sustaining for its entire lifetime.

There now exist an enormous number of publications on energy harvesters and energy-harvesting circuit interfaces, but much fewer studies that combine harvesters and interface electronics to create fully functioning energy harvesting systems [1-4]. For harvesting power from human movements, the list is even shorter. Of those combined harvester/electronics systems, many have one or more shortcomings. For example, some will deplete their stored charge during states of non-activity and therefore require an extra startup or bootstrapping procedure. Others do not provide a regulated output voltage and therefore are not readily compatible with modern electronic devices.

In this work, a fully functional, self-sufficient motional energy harvesting system is demonstrated, which features a unique energy harvesting transducer and a complete input-powered interface circuit, which together charge a thin-film battery from human movements.

SYSTEM DESIGN

Fig. 1 presents the block diagram of the system. The system consists of an omni-directional electrodynamic (magnetic) energy harvester, an input-powered interface circuit and a Li-ion polymer rechargeable battery. The kinetic energy from human movements is converted to electrical energy through the harvester, producing a quasi-chaotic time-varying voltage. This voltage is not able to charge the battery directly, so it is fed to the interface circuit, which rectifies and regulates the input to a constant dc voltage to charge the battery.

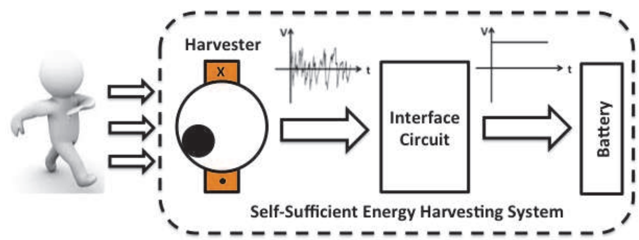

Figure 1. Block diagram of the self-sufficient energy harvesting system

Fig. 2 shows the prototype system. The interface power electronic circuit, excluding discrete components such as capacitors, diodes and inductors, was fabricated on silicon and packaged in a DIP40 package. The interface chip, the discrete components, and the rechargeable battery are assembled on a circular PCB and mounted on top of the harvester. The total volume of the prototype is about 100 cm^3.

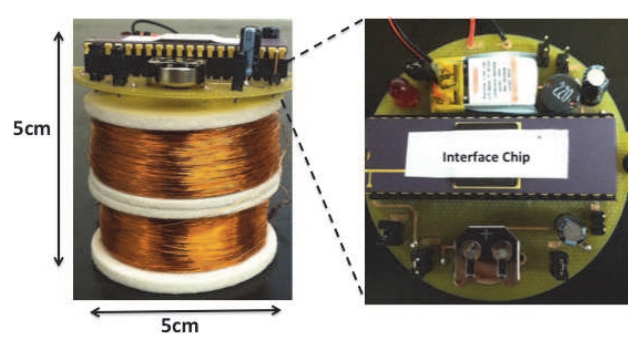

Figure 2. Photograph of the system

One feature of the proposed system is that it does not require any external power supply. Another feature is the zero standby power required by the input-powered interface circuit. Since the circuit is powered by its own ac input, it will be turned off with the absence of vibrational inputs. Together, these features not only allow indefinitely long intervals between two harvesting cycles, but also eliminate the need for additional startup circuitry, because the system will automatically "wake up" with vibrational input stimulations.

Energy Harvester

The harvester employs a spherical magnetic energy harvester design [5], where a permanent magnet (NdFeB) ball moves chaotically within a spherical housing wrapped with copper coils. When subjected to external vibrations/motions, the motion of the magnet ball induces a time-varying magnetic flux in the surrounding coil, and thus a voltage is generated according to Faraday's Law. If an electrical load (i.e. interface circuit) is connected across the two terminals of the coil, a current will flow to the load, converting mechanical energy into electrical energy.

Compared with electrostatic and piezoelectric energy harvesters, the electrodynamic harvester has the benefit of lower output impedance (a few Ω's to hundreds of Ω's). Additionally, the non-resonant harvester architecture is favorable for human movements because it responds to linear and rotational accelerations over a broad range of amplitudes and frequencies. However, the small output voltage level (few hundreds of mV to several volts) due to the limited practical size presents substantial technological challenges for the power electronic circuit design.

Interface Circuit

The interface circuit consists of two stages: a rectifier stage and a step-up dc/dc converter stage, as shown in Fig. 3. The rectifier stage converts the ac input voltage from the harvester to a dc voltage stored on the output capacitor. This dc voltage is normally too low to charge the battery and therefore the dc/dc converter is needed to boost the voltage to a usable voltage level. Meanwhile, the closed-loop control of the dc/dc converter provides output regulation, so that a constant output voltage is obtained at various input and load conditions.

There are actually two ac/dc rectifiers in the rectifier stage: primary rectifier and auxiliary rectifier. The primary rectifier converts the ac input to a dc voltage, which is then regulated by the dc/dc converter. An auxiliary rectifier is used to reduce the minimum operational input voltage of the dc/dc converter by providing a load-independent power supply voltage to the dc/dc controller. Both rectifiers employ the exact same design using half-wave active diodes, as shown in Fig. 4. Compared to a previous full-wave rectifier topology [7], a half-wave topology has been shown to deliver more power to the load in magnetic energy harvesting circuits where diode forward voltage drop is significant [8]. The comparator in the active diode is input-powered by connecting the power supply to the input through a diode D_1. The diode prevents turn-on of the parasitic diodes (silicon substrate to n-well) when the input is lower than the circuit ground.

The goal of the dc/dc boost converter is to provide a regulated dc voltage (V_{out}) for battery charging (Fig. 3). Compared with a previous dc/dc converter design [9], a level shifter is introduced to reduce the conduction loss of the switching transistor (M_1) by increasing the voltage swing of the switching pulse (V_{osc}). Transistor M_2 cuts off the resistor divider to avoid leakage current during standby mode.

The rectifiers and dc/dc converter were fabricated on silicon using an On Semi 3M-2P 0.5-μm CMOS process. The micrograph of the chip is shown in Fig. 5. The active die area is 0.05 mm^2 (115 μm × 440 μm) for the rectifier stage and 0.06 mm^2 (127 μm × 447 μm) for the dc/dc stage. Table 1 lists all the other discrete components used in the interface circuit except for the circuit chip.

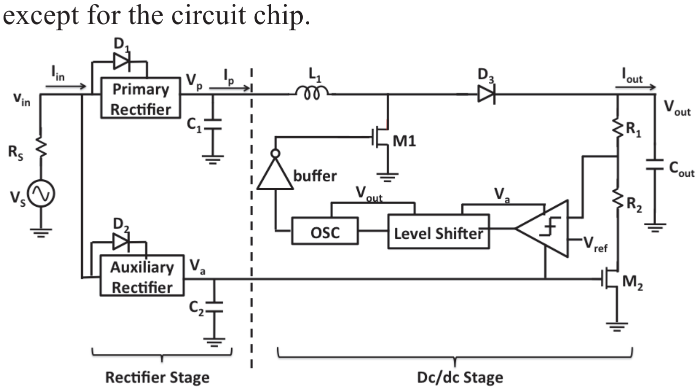

Figure 3. Block diagram of the interface circuit

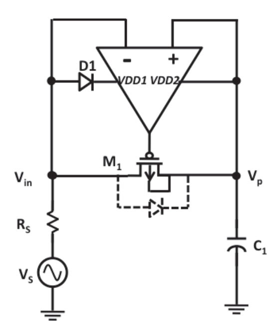

Figure 4. Schematic of the primary rectifier

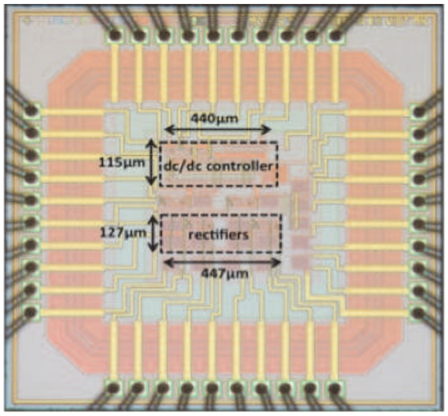

Figure 5. Micrograph of the interface circuit chip

Table 1. List of discrete components in the system

Type	*Name*	*Implementation*
Inductor	L_1	22 µH
Diode	D_1 , D_2 , D_3	NSR0320 [6]
Capacitor	C_1 , C_2 , C_{out}	220 µF
Resistor	R_1, R_2	R1: 3 MΩ R2: 1 MΩ

Rechargeable Battery

A commercial Li-ion polymer rechargeable battery with nominal voltage of 3.7 V and maximum capacity of 65 mAh [10] is used as the storage reservoir of the system. The battery comes with a self-protection circuit to avoid over-charge or over-discharge, and therefore no additional battery management circuit is needed in the system design.

EXPERIMENTAL

The performance of the interface circuit is first characterized, and then the whole energy harvesting system is measured with real human movements.

Interface Circuit Characterization

To bench-top characterize the interface circuit, a 20 Hz sine waveform from a function generator is used to mimic the output of a low-frequency energy harvester with different ac input voltage amplitudes. The interface circuit is configured to charge the battery at a fixed 3.7 V_{dc}. The measured output power ranges from 45 µW for a 1.2 V_{pk} input up to 5.2 mW for a 3 V_{pk} input, as shown in Fig. 6.

The interface circuit requires a minimum input voltage to ensure both the rectifier and the dc/dc converter function correctly. This input threshold becomes higher when the dc/dc converter is input-powered, because the rectifier output must be large enough to supply the dc/dc converter. When a load is connected to the interface circuit, the minimum input is even higher, because of a larger voltage ripple at the rectifier output. In our circuit design, the auxiliary rectifier reduces the minimum input voltage by generating a supply voltage for the dc/dc converter with less voltage ripple. Fig. 7 shows a measured example that auxiliary rectifier (V_a) has less voltage ripple than the primary rectifier (V_p) at 7.5 kΩ resistive load. With a 3.7 V-battery load, the interface circuit functions with minimum input voltage of 1.2 V_{pk}, compared with 1.5 V_{pk} without the auxiliary rectifier.

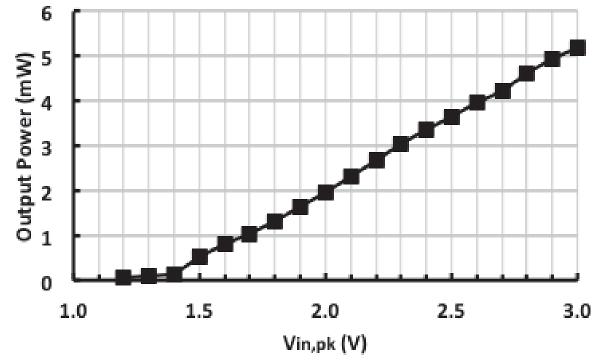

Figure 6. Power delivered to 3.7 V battery at different input voltage amplitudes (f =20 Hz)

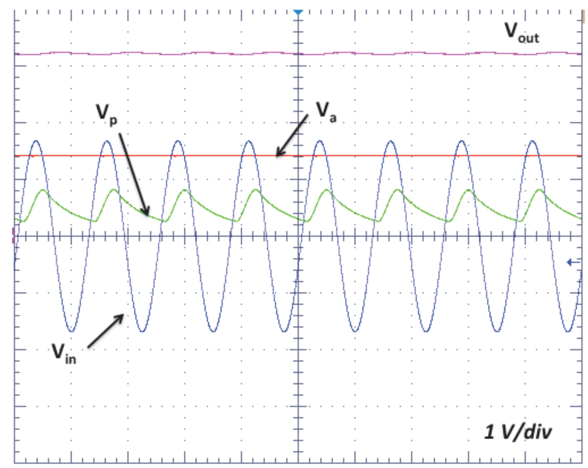

Figure 7. Measurement result at 7.5 kΩ load when input is a 20 Hz, 1.7 V amplitude sine wave

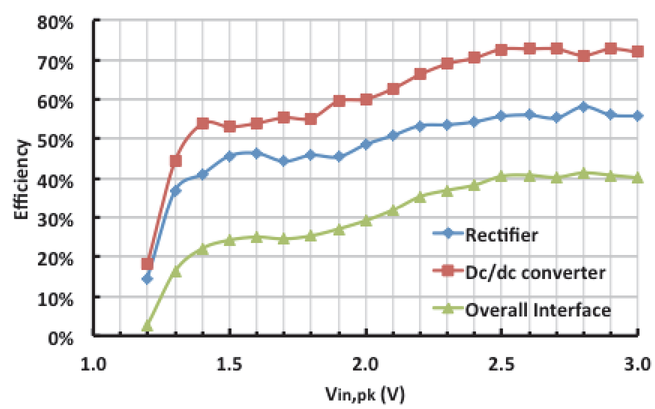

Figure 8. Circuit efficiency at different input voltage amplitudes (f =20 Hz) when charging a 3.7 V battery

Fig. 8 shows the bench-top measurement result of circuit power efficiencies of the rectifier stage, the dc/dc converter, and the overall interface circuit at different input voltage amplitudes. The efficiencies increase with the input amplitude because conduction loss decreases with smaller R_{ds}(on) of switching transistors (i.e. PMOS switches in the rectifiers and M1 in the dc/dc converter). The overall efficiency is above 40% for input voltages >2.5 V_{pk}.

Complete System Measurement

The energy reclamation performance of the complete system was measured on real human activities. In the experiment, the system was attached to a person who was walking, jogging on a treadmill and cycling on a cycling machine, so the speed of each activity is accurately controlled. Each activity type was tested for 20 minute duration and was repeated by attaching the system to different parts of the human body, including the ankle, wrist, and arm. To quantify the harvested energy, the battery voltage was measured before the activity and every 5 minutes during the activity. Using separately measured battery charging curves (voltage vs. state of charge), the total energy delivered from the system to the battery is estimated.

Fig. 9 shows the estimated energy delivered to the battery when the system was mounted on the ankle for three different activities. The energy delivered increases almost linearly with the time of human movements. The average harvested power can be estimated by calculating the slope of the line.

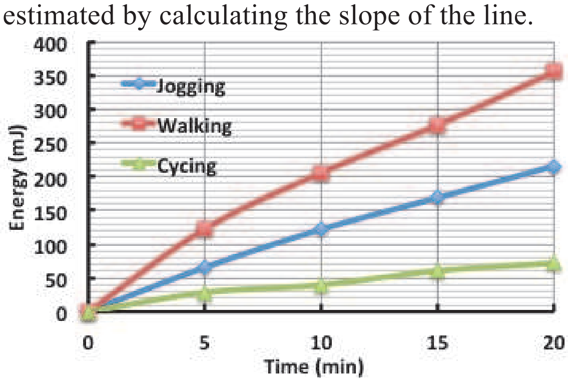

Figure 9. Energy delivered to the battery for the system mounted on the human ankle

Table 2 summarizes the other measurement results. The average power delivered to the battery ranges from 60 µW to 300 µW. Interestingly, when mounted on the ankle, the maximum power of 300 µW occurs for walking as opposed to running. Due to the relatively small upper-body vibrations, no significant power is measured at the wrist and arm during walking and cycling.

Table 2. Measured average power delivered to the battery during human movements.

	 **Ankle**	 **Wrist**	 **Arm**
Jogging (4mph)	180 µW	260 µW	210 µW
Walking (2.5mph)	300 µW	--	--
Cycling (22mph)	60 µW	--	--

CONCLUSION

A complete self-sufficient energy harvesting system is demonstrated and characterized. The system successfully scavenges and converts mechanical energy from daily human movements to electrical energy for charging a battery, with a maximum average power delivery of 300 µW during walking when mounted on the ankle. When there is no activity or the input energy is too low, the system enters standby mode with zero power consumption. Future work is to reduce the size of the system and further improve the output power.

ACKNOWLEDGEMENT

This work was supported in part by Texas Instruments via a fellowship for Yuan Rao.

REFERENCES

[1] T. Galchev, J. McCullagh, R. L. Peterson, and K. Najafi, A vibration- harvesting system for bridge health monitoring, *PowerMEMS*, pp. 179–182, 2010.

[2] A. Rahimi, O. Zorlu, H. Kulah, and A. Muhtaroglu, An interface circuit prototype for a vibration-based electromagnetic energy harvester, *Proc. Int. Conf. Energy Aware Comput.*, pp. 1–4, Cairo, Egypt, Dec. 2010.

[3] M. Marzencki, Y. Ammar, and S. Basrour, Integrated power harvesting system including a MEMS generator and a power management circuit, *Sens. Actuat. A: Phys.*, vols. 145, pp. 363–370, 2008.

[4] A. Rahimi, O. Zorlu, A. Muhtaroglu and H. Kulah, Fully self-powered electromagnetic energy harvesting system with highly efficient dual rail output, *IEEE Sensors Journal*, vol. 12, no. 6, pp. 2287-2297, 2012.

[5] B. J. Bowers and D. P. Arnold, Spherical rolling magnet generators for passive energy harvesting from human motion, *J. Micromech. Microeng*, vol. 19, 094008, 2009.

[6] On Semiconductor NSR0320 20V 1A low VF Schottky diode http://www.onsemi.com/PowerSolutions/product.do?id=NSR0320MW2T1G Webpage accessed on September 15, 2012.

[7] Y. Rao and D. P. Arnold, An input-powered active ac/dc converter with zero standby power for energy harvesting applications, *ECCE*, pp. 4441-4446, 2010.

[8] Clare. L. R, Burrow. S.G. Half-wave rectifiers offer advantages for vibration energy harvesters, *Electronics Letters*. vol. 46, pp. 1623-1624, 2010.

[9] Y. Rao and D. P. Arnold. An input-powered vibration energy harvesting interface circuit with zero standby power. *IEEE Transactions on Power Electronics*. vol. 26, pp. 3524-3533, 2011.

[10] Tenergy Li-ion polymer 3.7V 65mAh rechargeable battery, http://www.tenergy.com/30117 Webpage accessed on Sept. 15, 2012.